



Transiting planets and brown dwarfs in star forming regions and young open clusters

Suzanne Aigrain¹, Jonathan Irwin¹, Simon Hodgkin¹, Aude Alapini¹, Leslie Hebb², Estelle Moraux¹, Mike Irwin¹

and the Monitor Collaboration

¹Institute of Astronomy, University of Cambridge, UK; ²Johns Hopkins University, Baltimore, USA



suz@ast.cam.ac.uk

Abstract

We have undertaken since 2004 a photometric monitoring survey of a dozen star forming regions and open clusters aged between 1 and 200 Myr using wide-field optical cameras on 2 to 4m telescopes worldwide. The primary goal of the project is to search for close-in planets (and brown dwarfs) at young ages through the detection of transit events. Such detections would provide unprecedented constraints on planet formation and migration time-scales, as well as on evolutionary models of planets and brown dwarfs in an age range where such constraints are very scarce. Additional science goals include rotation period measurements and the analysis of other forms of variability such as flares and accretion-related variations. In this poster, we summarise the motivation behind and the design of the survey, and sketch out the predicted impact of the program once completed. Details of the data processing and photometric precision achieved are given, and we present preliminary results from observations to date and plans for follow-up observations.

More details are available on the Monitor webpage: <http://www.ast.cam.ac.uk/~suz/monitor/monitor.php>

Survey design

Target selection: About 10 target clusters were selected on the basis of youth, richness, proximity and compactness, as well as the existence of a known low-mass PMS population. We have observed or are scheduled to observe 8 of those by the end of 2005B (see Table 1 below right), and will apply to survey the remainder over the next few semesters.

Observing strategy: We use one 2m class and one 4m class telescope in each hemisphere, each equipped with wide-field optical imagers. Depending on the availability of service mode observing on the telescopes in question, we have opted for either a standard 'blocks of nights' strategy or an innovative 'randomised blocks' of 1-2 hours strategy that maximises the sensitivity to longer periods while making use of poor observing conditions few other programs can contend with.

Monitoring is carried out in i' (or I when i' is not available) with simultaneous V-band monitoring for the Orion Nebula Cluster (ONC) to maximise our ability to discriminate between eclipses and other forms of variability. We also take Hot Images every ~2 hours for the INT and CTIO targets, as well as deep exposures in 1 complementary filter (R or g') for the clusters for which deep CMDs are not already available in the literature (M34, M50, NGC2362, H & C Per).

Exposure times are adjusted to reach SNRs of at least 30 down to the Hydrogen burning limit while minimising readout overheads and keeping the time sampling to 15 min or better. When necessary to cover most of a given cluster, a mosaic of several pointings is used.

Data processing: All data reduction (bias subtraction, flat fielding, astrometric and photometric calibration) is done automatically using the Cambridge Astronomical Survey Unit (CASU) pipeline (Irwin & Lewis 2001). We then perform list driven aperture photometry, using variable aperture sizes depending on the brightness of the stars being measured. Finally, we apply a systematics correction procedure that corrects for trends common to many light curves by computing the residuals from the light curve median for each star in each frame, then producing a map of residuals versus position on the image for each frame. We then fit a 2-D polynomial to this map and subtract the fit from each star's light curve. Our pipeline, together with our experiments with a number of systematics removal / trend filtering algorithms available in the literature, will be described in an upcoming paper (Irwin et al. 2005a, in prep).

Photometric precision: Typically, we reach relative precisions of 2-3 mmag for our brightest targets in each cluster, and better than 1% over nearly 4 magnitudes, as illustrated in the case of M50 in Figure 3 (right).

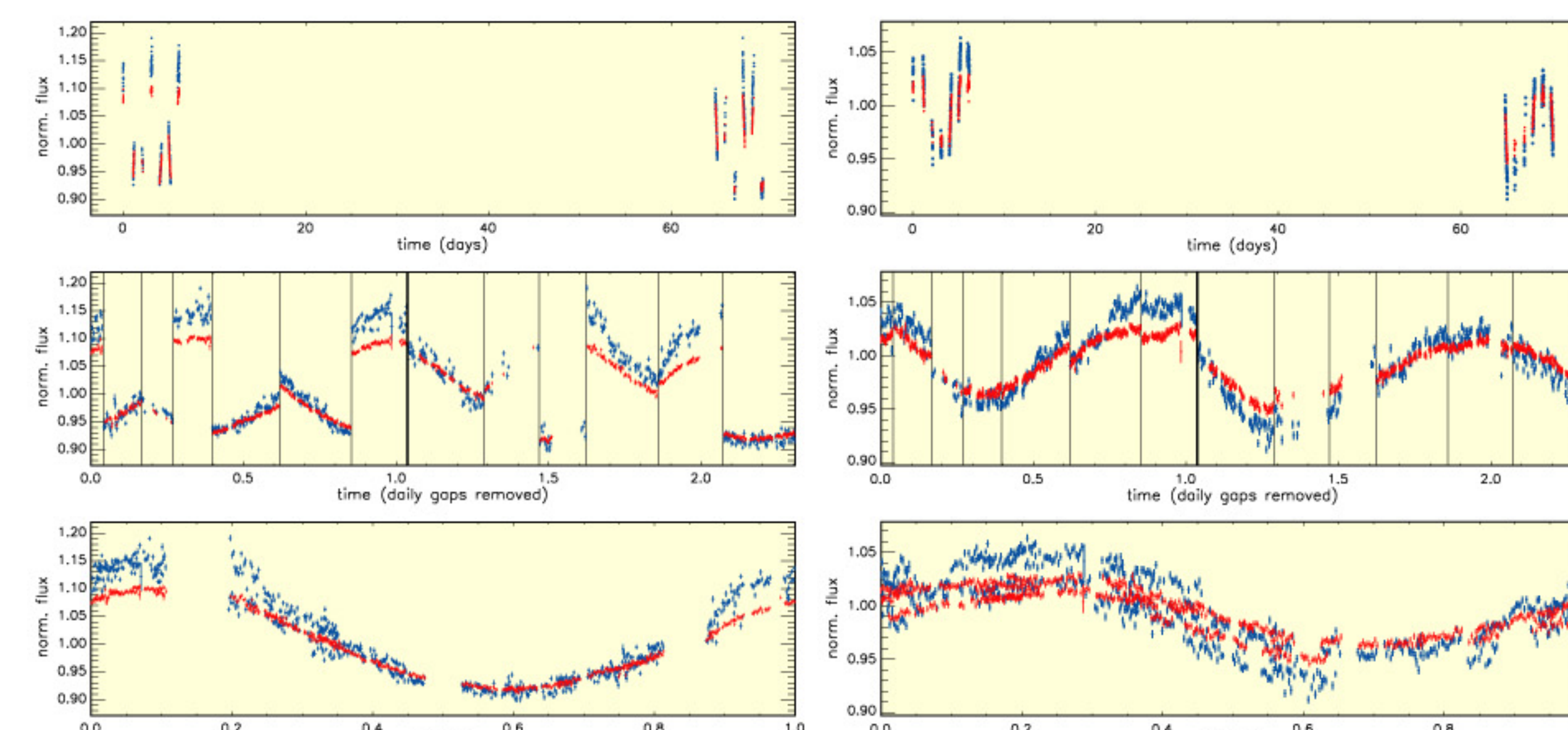


Figure 4: Two examples of rotational modulation from the central chip of the ONC field.

Top: Full *i*-band and *V*-band light curves.

Middle: Light curves with daily gaps removed (vertical lines mark daily gaps, the thick lines marks the gap between the two runs).

Bottom: Light curves folded at the detected *i*-band period of 0.84 and 1.5 days respectively. The latter are in excellent agreement with the periods identified by Herbst et al. 2002 for these stars (0.85 and 1.5 days respectively) though shape and amplitude have since evolved. Note larger amplitudes and increased short term variability in *V*, as well as the change in amplitude between the first and second runs in the left panel.

Rotation periods

We search for rotation periods using our own sine-curve fitting algorithm, which is run on the light curves of all objects classified as stellar and unblended that do not repeatedly fall on low confidence regions of the detector. The best fit is accepted if the reduced chi squared of the light curve is significantly improved by subtracting a smoothed version of the light curve phase folded at the best-fit period. We also discarded any cases where the phase coverage was less than 50%, which we found removed most spurious or uncertain detections.

In the ONC, we have tentatively measured rotation periods between a few hours and 20.0 days in ~800 of the 2000 objects in our field (see examples in Figure 4 above), an increase by a factor ~40 on the number of previously published values (Herbst et al. 2002, Stassun et al. 2000). We are particularly sensitive at the short period end thanks to our very high time sampling rate (3.5 min). We can also study the temporal evolution and temperature profiles of the spots responsible for the modulation through amplitude changes between our two runs separated by 2 months, and differences between the *i*' and *V* filters respectively.

We have also run period searches in the other clusters observed to date, though we are restricted to shorter periods due to the smaller time span of our observations. We are currently in the process of assessing our sensitivity to aliasing and any other biases and completeness limits before computing period distributions for each dataset. These will provide an unprecedented insight into the rotational evolution of (very) low mass stars over the first 200 Myr. In the case of M34, for which we are carrying out the first membership study at low masses (Irwin et al. 2005b, in prep), we will also use the presence of rotational modulation as a membership indicator (see Figure 5 [right]).

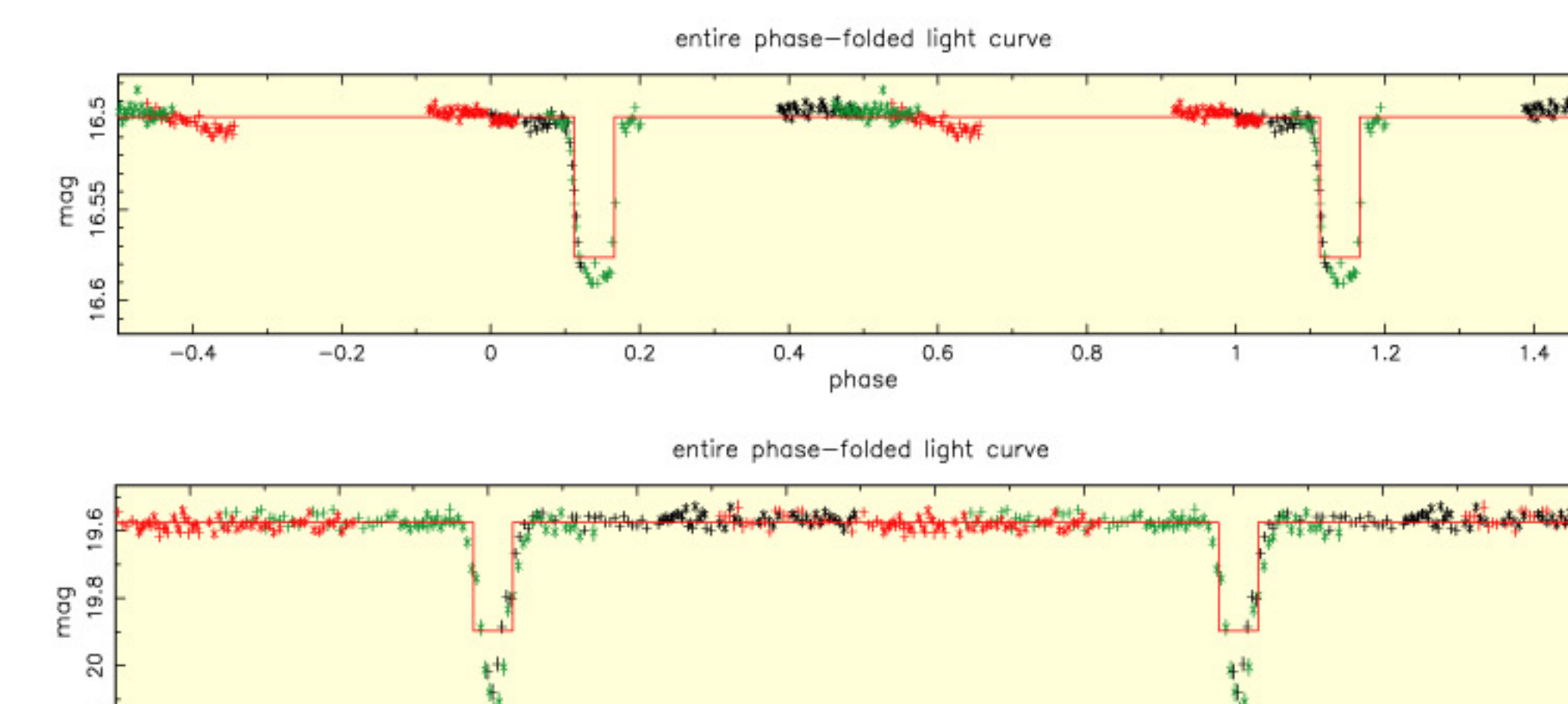


Figure 7: Two examples of eclipse candidates in the M50. These *i*-band light curves have been phase folded at the best fit periods of 1.857 and 0.766 days respectively. The symbols and colours have the same meaning as in Figure 6 (top-right), with two-night CTIO runs separated by 5 nights in Feb 2005. Secondary eclipses can be seen in the top panel. The primary and secondary eclipse depths can be used to deduce a flux ratio of 0.16 for the two components, which, combined with the system apparent *R* and *I* magnitudes, implies approximate masses of 0.73 and 0.41 M_{\odot} (following the models of Baraffe et al. 1998, at the age and distance of the cluster). The bottom panel shows grazing eclipses whose depth suggests a near equal mass system with individual masses of ~0.22 M_{\odot} .

Introduction

Background: Though well over 100 extrasolar planets are known today, the vast majority orbit field stars with poorly determined ages. In particular, this is true of all 8 known transiting exoplanets, which are the only cases for which radii and (in the cases of HD209458b and TrES1b, whose secondary eclipses have been detected, Deming et al. 2005, Charbonneau et al. 2005), surface effective temperatures are known.

The detection of a transiting exoplanet orbiting a star of known age would thus constitute the first firm anchoring point for evolutionary models of extrasolar planets. Over the last few years, several transit surveys (e.g. Explore OC, von Braun et al. 2004) have been targeting open clusters, whose members have relatively well known ages. However, all have concentrated on 'middle aged' clusters (several hundred Myr and older), and no confirmed discoveries have been reported to date.

Young transiting exoplanets: The Monitor project is targeting nearby star forming regions and open clusters in the so far uncharted 1 to 200 Myr age range, with the aims of detecting the first young transiting exoplanet(s) and of providing unprecedented observational constraints over the early evolution of these objects. In our youngest targets (<10 Myr), a detection would take added significance, as it would have implications for the disk evolution, planetesimal formation and migration timescales that are of fundamental importance for our understanding of how planets form.

Ultra low mass eclipsing binaries: We are also interested in searching for very low mass eclipsing binaries, with at least one sub stellar or very low mass star component. Evolutionary models in this age and mass range are notoriously uncertain, as has been illustrated by the controversy over recent detections of ultra-low mass visual binaries in young associations (Close et al. 2005). While brown dwarfs in high mass ratio or wide binaries are known to be rare from radial velocity and high resolution imaging surveys, our program is ideally suited to detect them in the near-equal mass, small separation area of parameter space, which has not been surveyed thoroughly.

Additional science: The light curves we are collecting are ideally suited to search for stellar rotation periods and to study short term (accretion related) or flare-like variability. Studying these effects is not only of immediate scientific importance, it is an integral and necessary part of the transit/eclipse search process, as transits can easily be mimicked or obscured by other forms of variability.

The motivation behind this survey and its expected impact will be detailed in an upcoming paper (Aigrain et al. 2005, in prep).

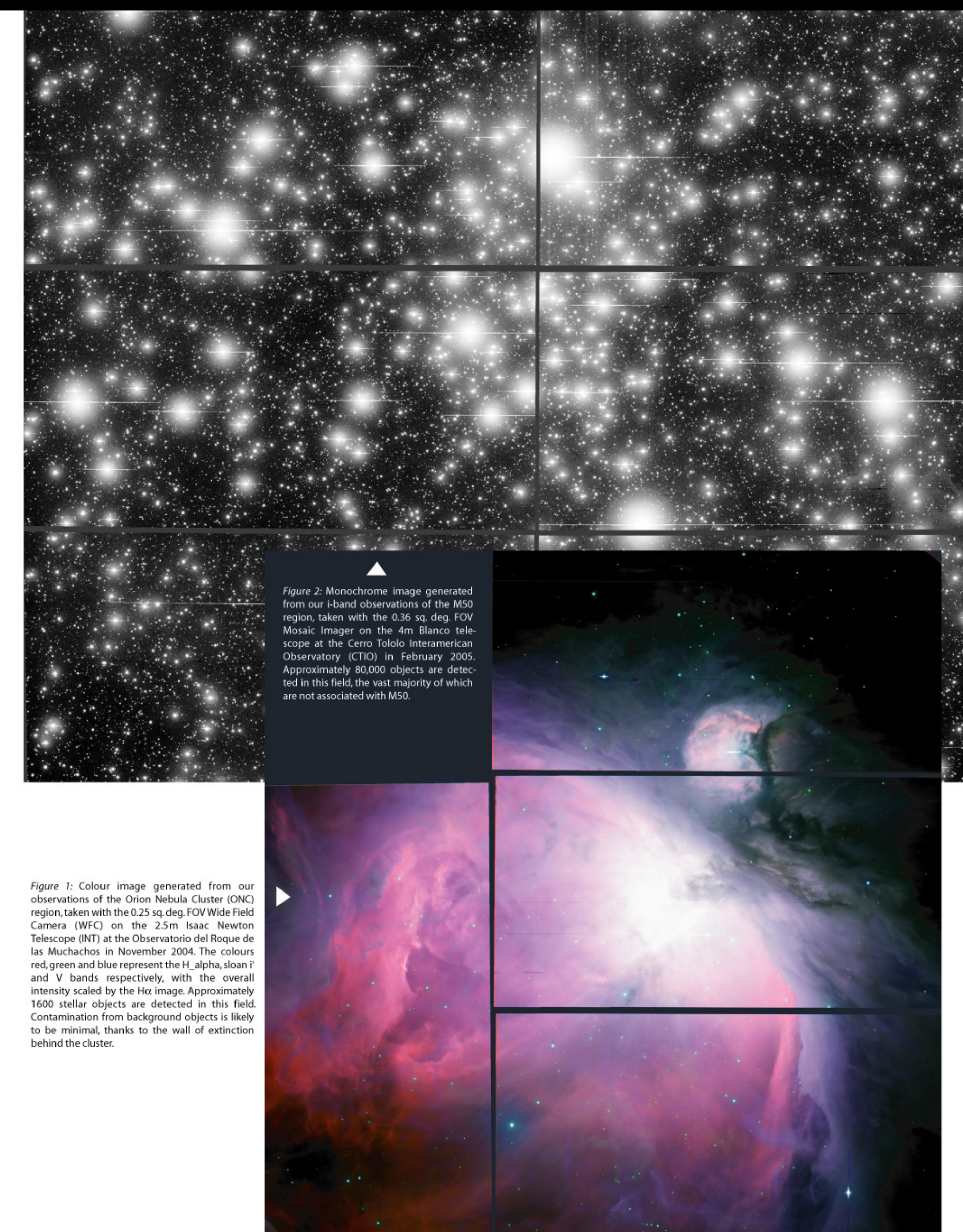


Figure 2: Monochrome image generated from our *i*-band observations of the M50 region, taken with the 0.36 sq. deg. FOV Mosaic Imager on the 4m Blanco telescope at the Cerro Tololo Inter-American Observatory (CTIO) in February 2005. Approximately 80,000 objects are detected in this field, the vast majority of which are not associated with M50.

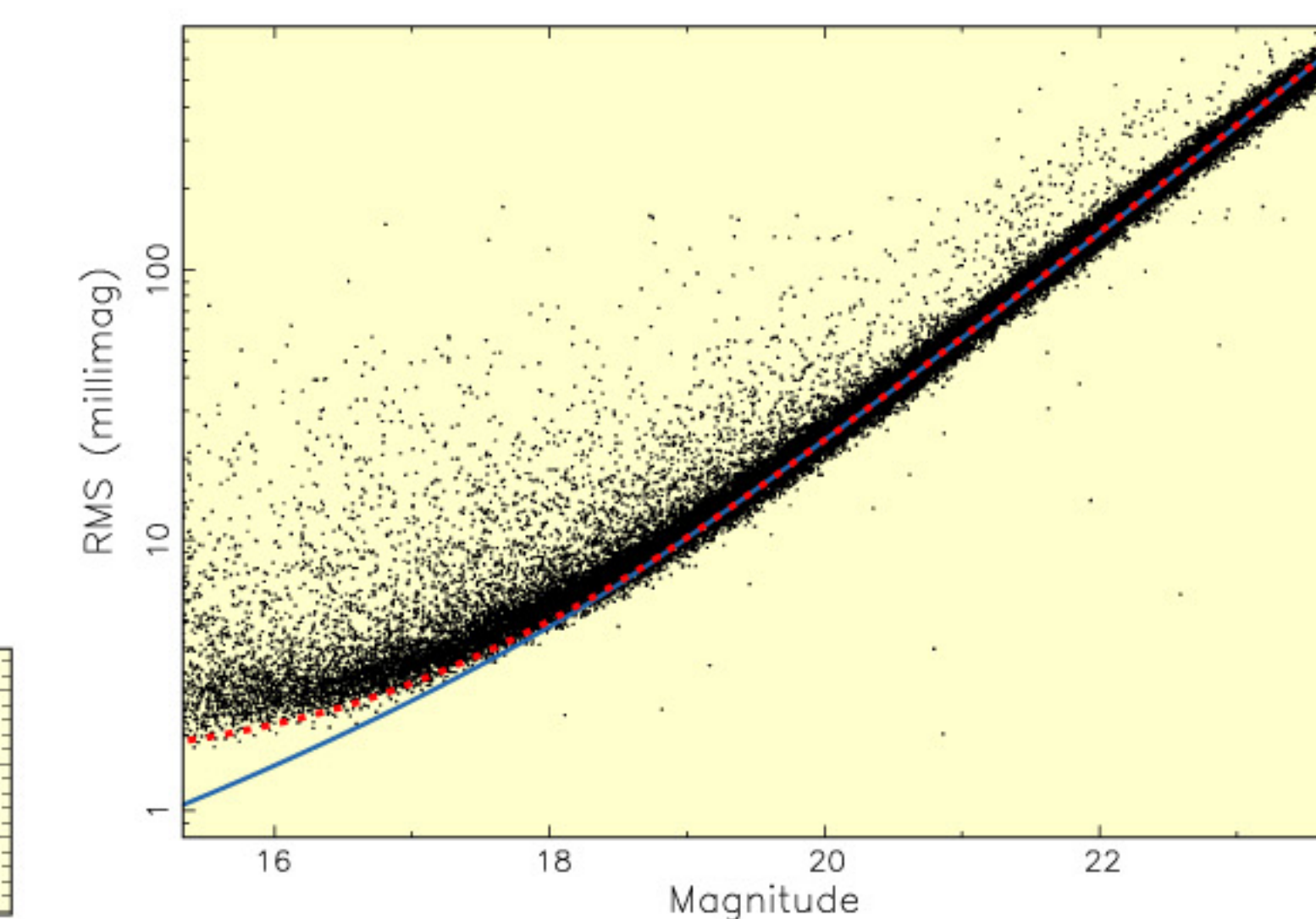


Figure 3: RMS scatter versus magnitude for all objects in the M50 field classified as stellar, obtained for the Feb 2005 CTIO data. The solid blue line shows the expected RMS, calculated as the quadrature sum of contributions from readout noise, sky noise in the photometric aperture and object photon noise. A dotted red line shows the same with a constant equal to 1.5 mmag added to account for residual systematic effects.

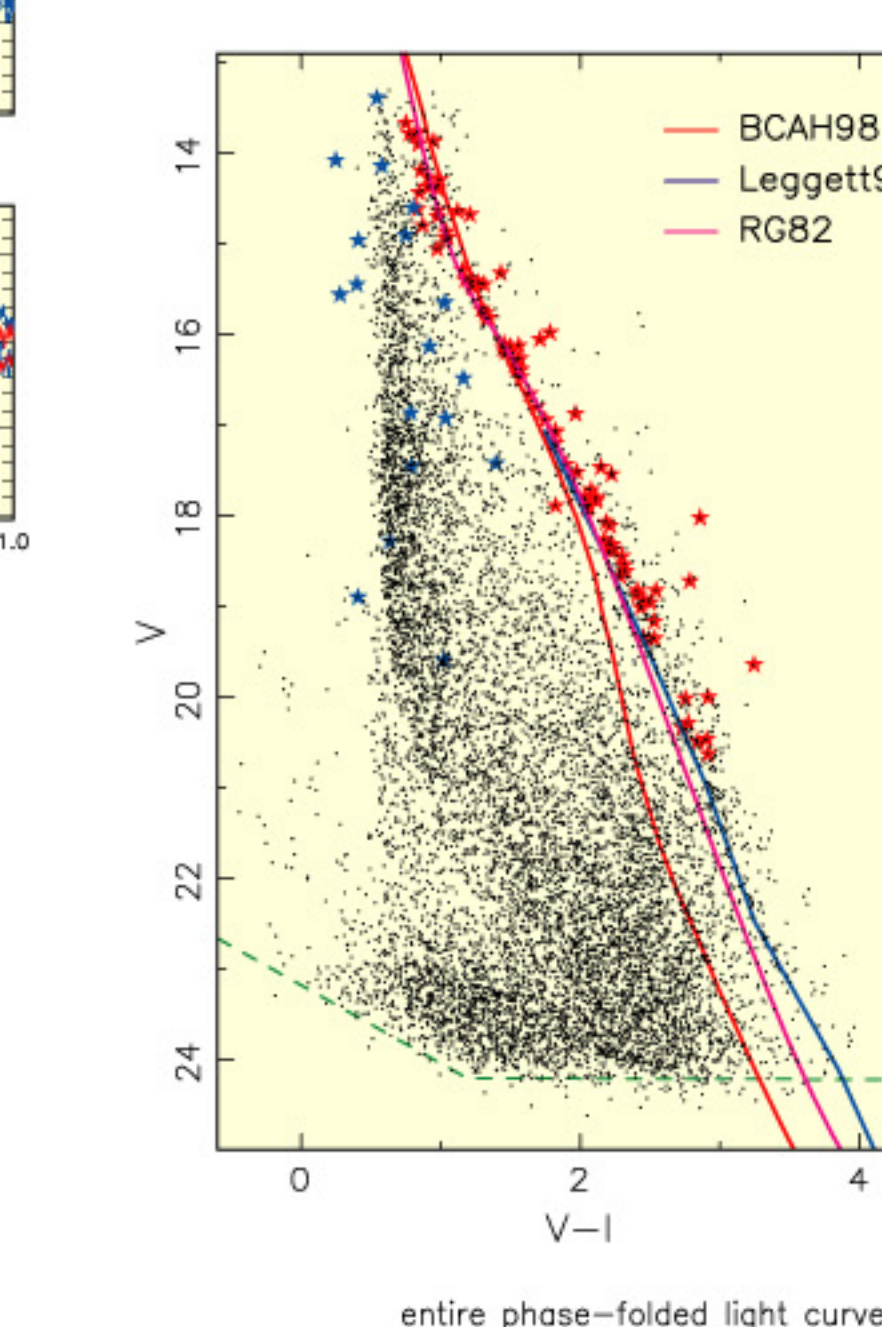


Figure 5: Colour-magnitude diagram for M34 generated from our Nov 2004 INT data, with the isochrones of Barraffe et al. 1998 (solid red), Leggett 1992 (dashed green), and Gilmore 1982 (empirical) in red, blue and pink respectively. Star symbols represent objects with sine-like periodic variations in their light curves. The fact that the majority of those fall on the cluster sequence (red symbols) illustrates the potential use of rotational modulation as a membership indicator. Note the lack of periodicity detections at the faint end, reflecting (i) this CMD was generated from stacked images much deeper than any individual image, and (ii) we are currently using rather stringent detection thresholds.

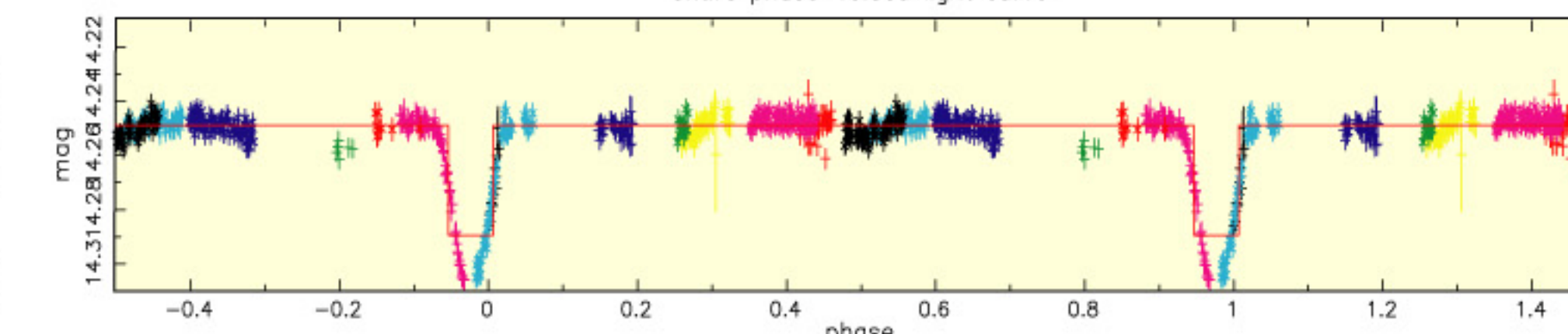


Figure 6: Example of an eclipse candidate in the ONC. This *i*-band light curve has been phase folded at the best fit period of 2.649 days after filtering out long-term variations using a pseudo-highpass filter. Different plotting symbols (+ and x respectively) were used for data from the November 2004 and December 2005 INT runs, while each night in a given run is identified by a different colour. The *V*-band light curve shows eclipses of similar depth and shape. This object's optical and near-IR colours indicate a primary mass of ~0.3 M_{\odot} . Following the prescription of Seager & Mallen-Ornelas 2003, we deduce primary and companion radii of 1.32 and 0.25 R_{\oplus} (the former in agreement with theoretical expectations for a star of such mass at 1 Myr), an orbital distance of 4.2 R_{\oplus} and hence a total system mass of ~0.302 M_{\odot} . The companion could therefore be of substellar or planetary mass.

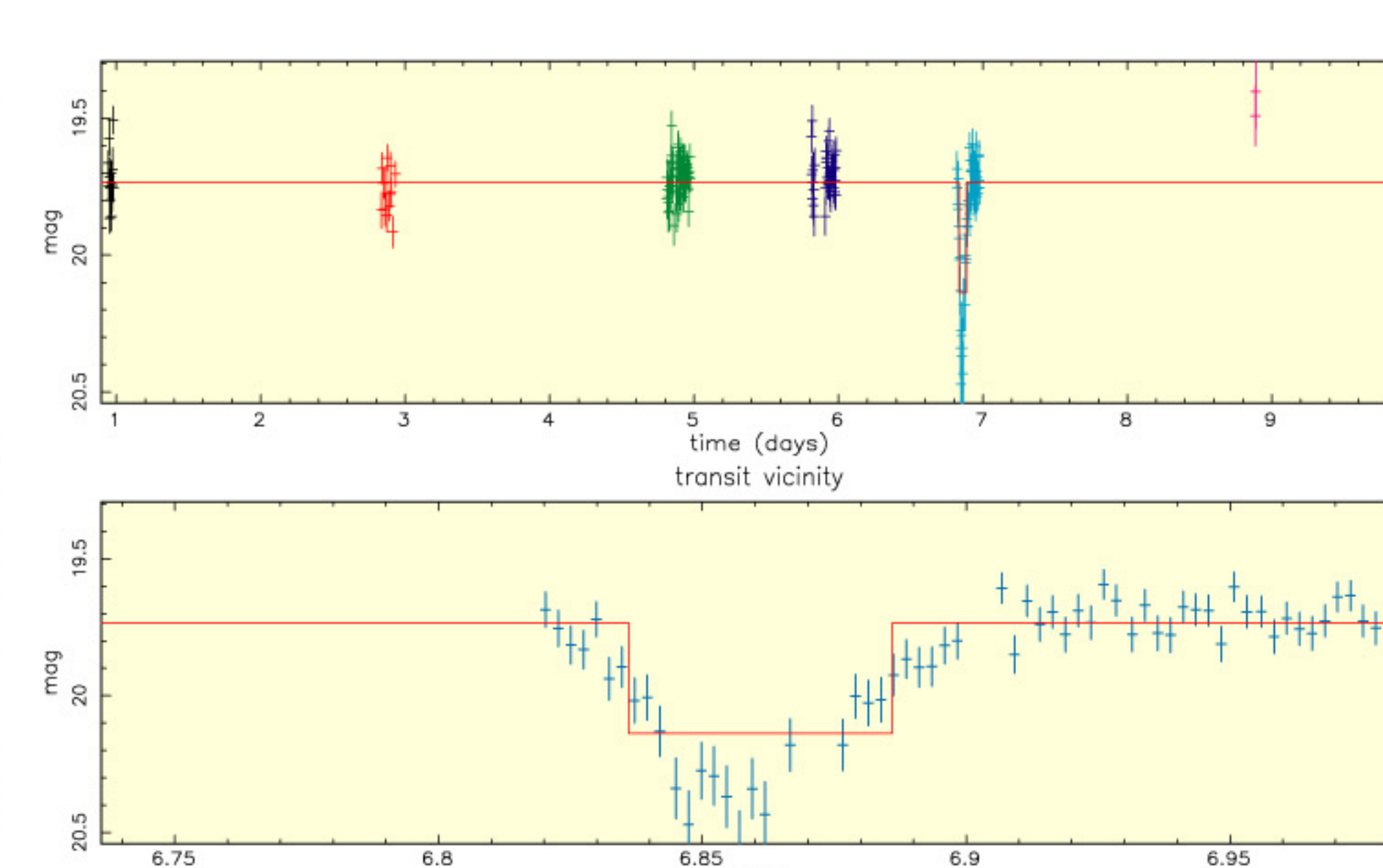


Figure 7: An example eclipse candidate in M34, with the same plotting convention as in Figure 6 for a single INT run in Nov. 2004. The top panel shows the full *i*-band light curve, the middle panel focuses on the single eclipse, which may or may not have a flat bottomed part. While the period is unknown, this object falls near the bottom of the cluster sequence (*I*=19.27, *V*=22.08, implying a mass of ~0.16 M_{\odot}), and will be very interesting if membership is confirmed.

Cluster	Age	M-m Myr mag	Telescope/Instrument	Observations	Filters	Exposure time	Area	Cycle time	Mass range	No. members	Expected no. detections		
				completed, in progress or scheduled		s	sq. deg.	min	M_{\odot}	in survey area	EBs	planets	
ONC	1	8.16	INT/ WFC	5n 11/04 5n 01/04 10n 2005B	i', V	30, 60	0.25	3.5	0.02-0.65	~1600	21.5	3.8	
NGC 2362	7	11.0	CTIO4m/ Mosaic	6n 02/05 8n 2005B	i	75	0.36	7.5	0.02-1.00	1000	7.2	1.3	
h & X Per	13	11.85	CFHT/ MegaCAM	40n 2005B	i'	2x60	1.0	10	0.07-1.05	8000	44.8	1.0	
NGC 2457	30	8.4	ESO2.2m/ WIFI	100n 2005B	I	120	0.5	7.5	0.04-1.00	300	1.5	0.3	
IC 4665	50	8.3	CFHT/ MegaCAM	40h 2005A	i	120	4.0	15	0.04-0.90	300	1	0.2	
Blanco 1	100	7.1	ESO2.2m/ WIFI	50h 2005B	I	120	1.00	15	0.04-0.90	320	0.9	0.3	
M50	130	10.5	CTIO4m/ Mosaic	8n 2005B	i	75	0.36	7.5	0.06-0.85	1700	4	1	
M34	180	8.7	INT/ WFC	5n 11/04	i', V	30, 60	0.25	3.5	0.04-1.00	~250	1.1	0.2	
				CFHT/ MegaCAM		40h 2005B	i	150	1.00	10	0.55-0.90	~400	
Total										8.7	0.02-1.05	13870	82
													8.1

Table 1: Clusters targeted so far with observational details and expected detection rates. Note that the last four columns are loose estimates and are meant more for inter-comparison than absolute purposes

Eclipses

Expectations: We have adapted the method developed by Gaudi et al. 2005 to estimate the expected number of detections from transit surveys in the field to the case of Monitor, using assumptions specific to the clustered, very young and low-mass nature of this project's targets. We take into account the mass range and number of members (potential primaries) surveyed, and for each primary mass bin we compute the expected incidence, period and mass distribution of companions (including stellar/substellar and planets, using the latest available distributions), and the alignment probability, and hence the number of eclipsing systems. Those are considered detectable if the photometric precision per data point at that mass and the average number of in-transit data points for such a system and time sampling result in a signal-to-noise ratio^a (SNR) of 10 or more.

These estimates are listed in Table 1 (above) and will be presented in more detail in Aigrain et al. (2005 in prep). In most cases, we are limited over the entire primary mass range by companion incidence and alignment probability rather than signal to noise (in the